

A theoretical study of the hydrates of $(\text{H}_2\text{SO}_4)_2$ and its implications for the formation of new atmospheric particles

J.C. Ianni*, A.R. Bandy

Department of Chemistry, Drexel University, Philadelphia, PA 19104, USA

Received 16 December 1998; received in revised form 24 May 1999; accepted 24 May 1999

Abstract

Density functional molecular orbital theory was used at the B3LYP/6-311++G(2d,2p)//B3LYP/6-311++G(2d,2p) level of theory to study the hydrates of $(\text{H}_2\text{SO}_4)_2 \cdot n\text{H}_2\text{O}$ for $n = 0-6$. All clusters studied were composed of hydrogen bonded molecular complexes of H_2SO_4 , H_2O and contain no double ions. The energetics of the hydration reactions were also calculated. All the reactions producing $(\text{H}_2\text{SO}_4)_2 \cdot n\text{H}_2\text{O}$ ($n = 0-6$) from $\text{H}_2\text{SO}_4 \cdot n\text{H}_2\text{O}$ and H_2SO_4 are spontaneous. A chemical mechanism is given to possibly explain the growth of ultrafine (1–30 nm diameter) tropospheric and stratospheric sulfate aerosols. © 2000 Elsevier Science B.V. All rights reserved.

Keywords: Density functional theory; Hydrated sulfates; Atmospheric particles

1. Introduction

Hydrated sulfates play an important role in the formation of new atmospheric particles [1–12]. These new particles are known to influence the concentration of cloud condensation nuclei in the atmosphere [5,13–19]. Cloud condensation nucleation can alter the optical properties of clouds affecting the radiation budget of the earth and the temperature of the earth [2,8]. In addition, sulfuric acid hydrates are known to provide a surface medium for reactions, which can lead to ozone destruction in the Arctic and Antarctic stratosphere [5,20–23]. We believe many of these sulfates are actually (or were initially) composed of $(\text{H}_2\text{SO}_4)_2 \cdot 2\text{H}_2\text{O}$.

The study of the hydrates of $(\text{H}_2\text{SO}_4)_2$ is a continuation from a previous paper which concentrated on the hydrates of $\text{H}_2\text{SO}_4 \cdot n\text{H}_2\text{O}$, $n = 0-7$. Our previous paper [24] has shown that clusters of H_2SO_4 hydrates are composed of very strong hydrogen bonds and do not contain any ions except at $\text{H}_2\text{SO}_4 \cdot 7\text{H}_2\text{O}$. This conclusion is in strong contrast to previous papers that assumed that the properties of particles containing H_2SO_4 and H_2O could be obtained by extrapolation from the properties of the bulk-phase which consists primarily of ions. A primary focus of this study is to try to answer the very important question: Can $(\text{H}_2\text{SO}_4)_2 \cdot n\text{H}_2\text{O}$ form spontaneously from $\text{H}_2\text{SO}_4 \cdot n\text{H}_2\text{O}$? The primary reason for this question is the abundance of atmospheric sulfate aerosol measurements, which show a sulfuric acid to water ratio of 1:2 [25,26]. Why does this ratio always seem to be around 1:2? We will answer this question by showing a possible chemical mechanism for this

* Corresponding author. Tel.: + 1-215-895-1576; fax: + 1-215-895-1980.

E-mail address: jamesianni@netscape.net (J.C. Ianni).

Table 1
DFT results for the individual molecules

	Temperature (K)	E_{elec} (hartree/mol)	ZPVE (kcal/mol)	E_{Thermal} (kcal/mol)	S (cal/(mol K))
(H ₂ SO ₄) ₂	298	−1400.798494	49.8	57.0	109.5
	273			56.0	106.0
	248			55.1	102.3
	223			54.3	98.5
	198			53.5	94.6
(H ₂ SO ₄) ₂ ·H ₂ O	173	−1477.275869	65.2	52.8	90.5
	298			74.2	126.4
	273			73.0	122.0
	248			71.9	117.5
	223			70.8	112.9
(H ₂ SO ₄) ₂ ·2H ₂ O	198	−1553.754719	80.7	69.9	108.0
	173			69.0	102.8
	298			91.4	141.7
	273			90.0	136.7
	248			88.7	131.4
(H ₂ SO ₄) ₂ ·3H ₂ O	223	−1630.234749	96.5	87.4	125.9
	198			86.3	120.1
	173			85.2	114.1
	298			108.9	154.1
	273			107.3	148.3
(H ₂ SO ₄) ₂ ·4H ₂ O	248	−1706.713565	112.2	105.8	142.2
	223			104.3	135.9
	198			103.0	129.2
	173			101.7	122.2
	298			126.3	171.1
(H ₂ SO ₄) ₂ ·5H ₂ O	273	−1783.193706	128.0	124.5	164.5
	248			122.7	157.6
	223			121.1	150.3
	198			119.5	142.7
	173			118.1	134.8
(H ₂ SO ₄) ₂ ·6H ₂ O	298	−1859.674581	143.8	143.7	184.5
	273			141.6	177.2
	248			139.7	169.5
	223			137.9	161.5
	198			136.1	153.1
(H ₂ SO ₄) ₂ ·6H ₂ O	173	−1859.674581	143.8	134.5	144.2
	298			161.1	197.1
	273			158.8	189.0
	248			156.7	180.6
	223			154.6	171.8
(H ₂ SO ₄) ₂ ·6H ₂ O	198	−1859.674581	143.8	152.8	162.6
	173			151.0	152.9

ratio. It should also be noted that we have partly answered that question in our previous paper by showing that (H₂SO₄)₂·6H₂O can spontaneously form from H₂SO₄·6H₂O, but we will show in this paper that it is of little significance and is not responsible for the initial formation of ultrafine atmospheric aerosols.

2. Computational details

To gain insight into this problem we used high level density functional molecular orbital methods to investigate the energetics and molecular structures of (H₂SO₄)₂·*n*H₂O clusters from *n* = 0 to 6. These results were obtained with density functional

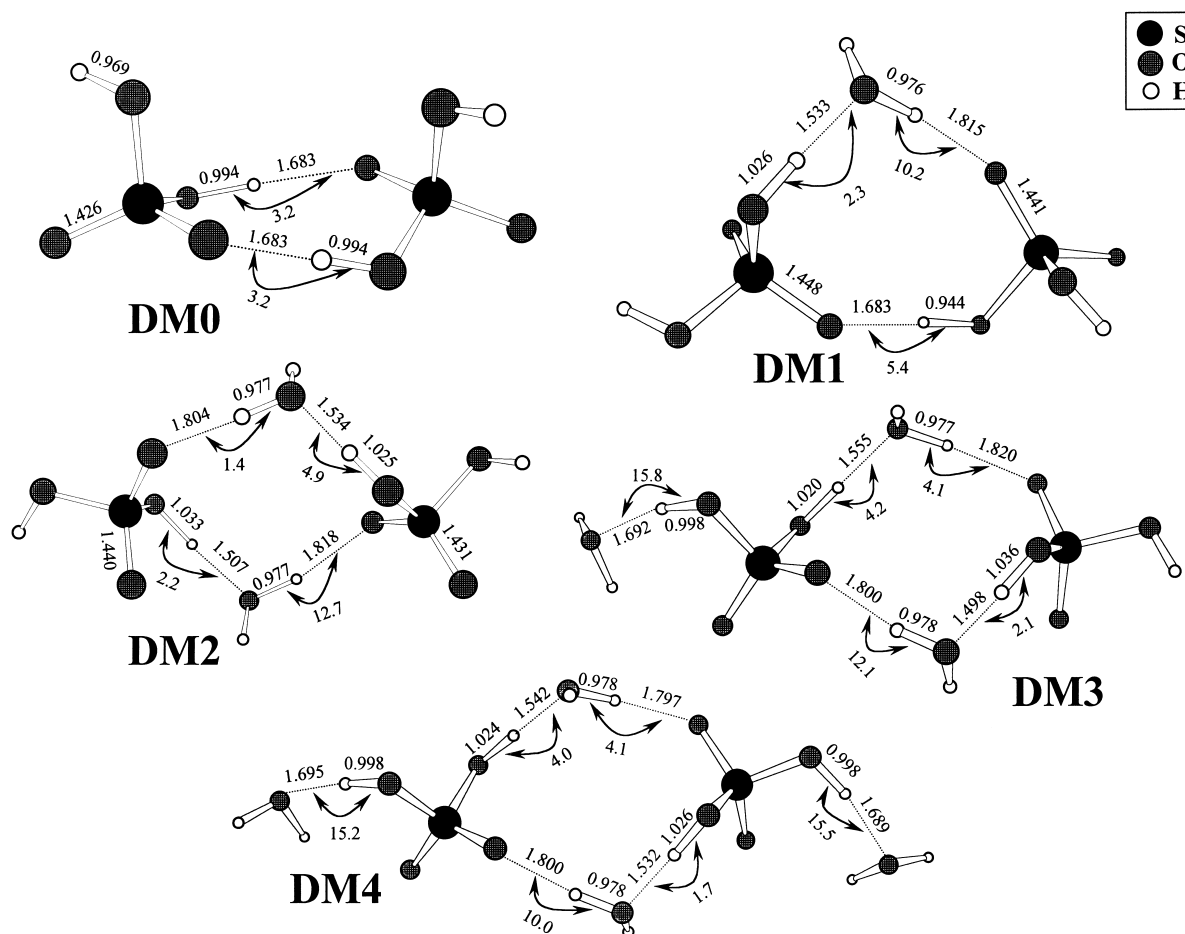


Fig. 1. Structures of $(\text{H}_2\text{SO}_4)_n\text{H}_2\text{O}$, $n = 0-6$ calculated at B3LYP/6-311++G(2d,2p)//B3LYP/6-311++G(2d,2p). Angles are in degrees and bond lengths are in Angstroms. Angles for hydrogen bonds are supplement angles: $180^\circ - \angle \text{O}-\text{H}\cdots\text{O}$.

methods at the B3LYP/6-311++G(2d,2p)//B3LYP/6-311++G(2d,2p) level of theory [27] as implemented in the GAUSSIAN 94 program [28]. We chose this level of theory because it is known to give good results for hydrogen bonded systems [29–33].

Free energies were calculated as follows:

$$\Delta G = \Delta H - T\Delta S,$$

$$\Delta H = \Delta E + \Delta(PV) = \Delta E + \Delta nRT,$$

$$\Delta E = \Delta E_c^0 + \Delta E_{\text{Thermal}},$$

$$\Delta E_{\text{Thermal}} = \Delta ZPVE + \Delta E_{\text{vib}} + \Delta E_{\text{rot}} + \Delta E_{\text{tran}},$$

where ΔG is the free energy change of the reaction,

ΔH the enthalpy change, Δn the change in moles of the reaction, R the gas constant, ΔS is the entropy change, ΔE the energy difference, ΔE_c^0 the difference in electronic energy at 0 K, $\Delta E_{\text{Thermal}}$ contains the difference in the zero-point vibrational energy at 0 K and ΔE_{vib} , ΔE_{rot} , ΔE_{tran} are the differences in vibrational, rotational and translational energies, respectively, at temperature T and 1 atm. Table 1 contains all the values required for the above free energy calculation. None of the vibrational frequencies were scaled due to the fact that the scaling factor for B3LYP is close to unity [34]. In addition, no basis set superpositional errors (BSSE) were computed since it has been demonstrated that B3LYP with very large basis

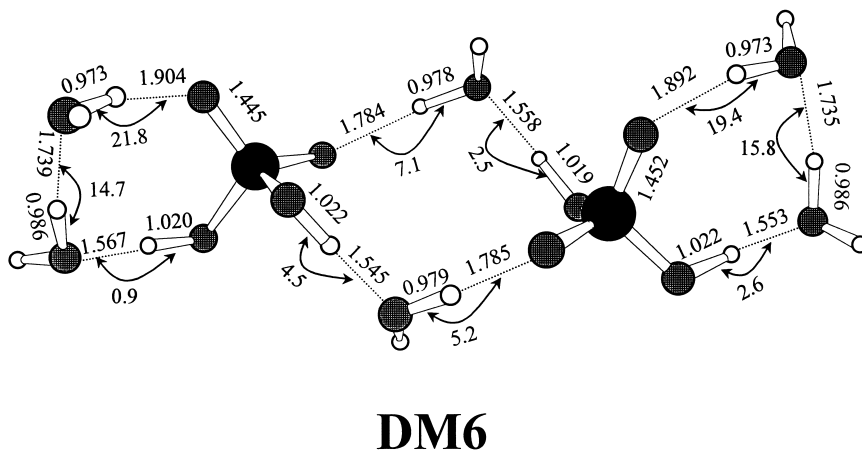
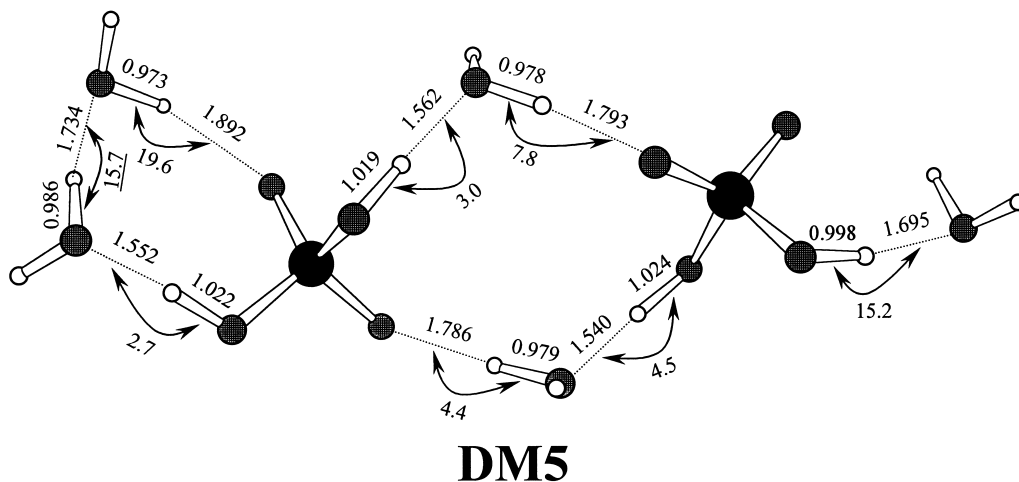


Fig. 1. (continued)

sets (such as the one used in this study) almost have a negligible BSSE error [33].

We have tried to find the global minima to the structures $(\text{H}_2\text{SO}_4)_2 \cdot n\text{H}_2\text{O}$ ($n = 0-6$) by starting at various geometries which maximize the hydrogen bond interaction between H_2SO_4 and H_2O . Maximizing the hydrogen bond interaction between H_2SO_4 and H_2O has been shown to be a good method to obtain structures that are excellent candidates for global minima [24]. All geometries were converged to the GAUSSIAN 94 standard convergence criteria. In most cases RMS and maximum forces were much lower. The energy in the SCF step was set to converge at 1×10^{-9} hartree. The minima were verified with a frequency analysis. Those structures that had one or

more negative frequencies were excluded from this study.

3. Results and discussion

3.1. Optimized geometries

For an accurate description of the hydrogen bonds, which are essentially holding these structures together as well as determining their geometry, we will be using hydrogen bond descriptors (HBD) in our discussion. The HBD will be enclosed in parenthesis and contain three values: (acceptor length, donor length, supplement angle). Acceptor length will show the

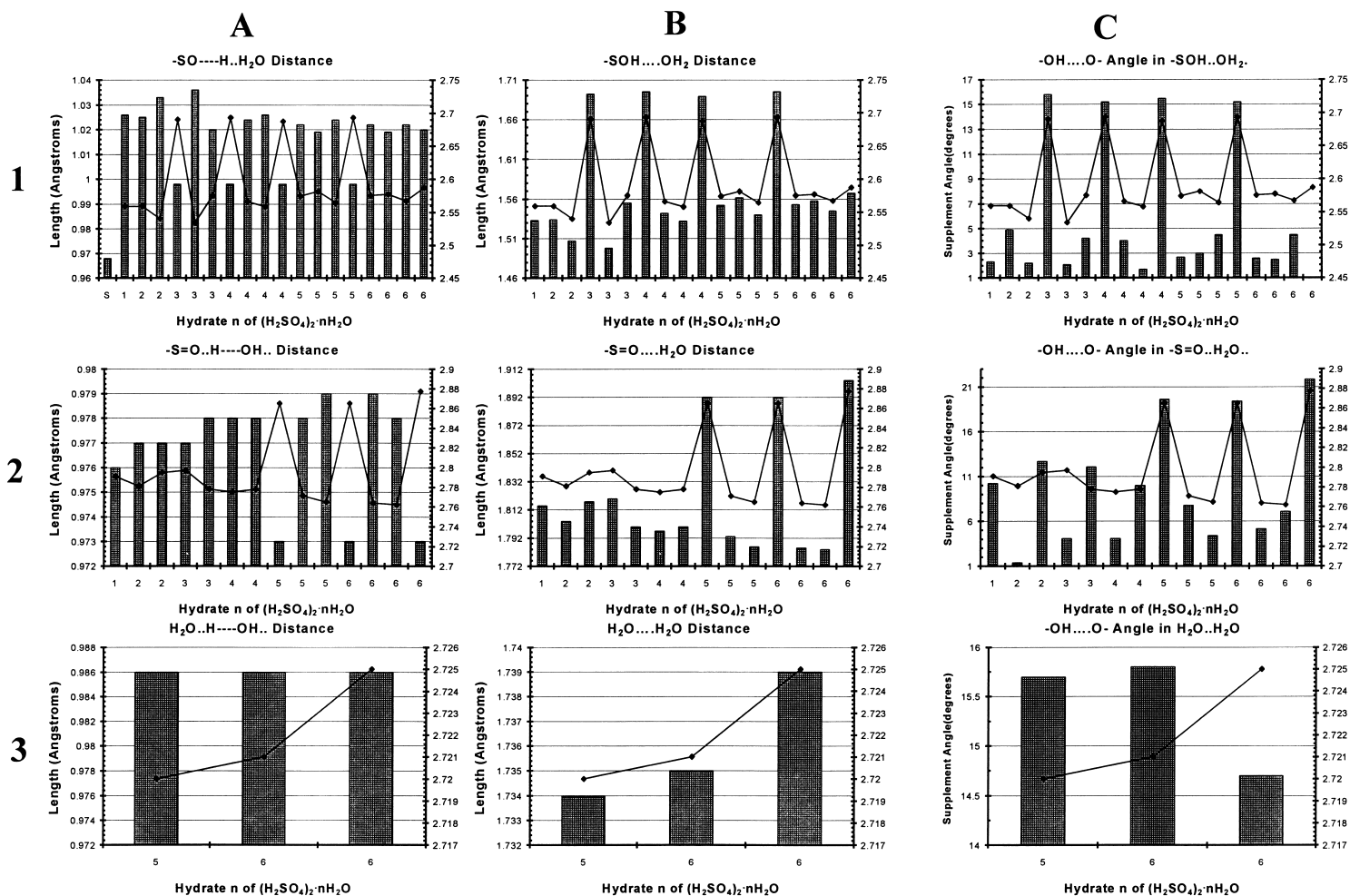


Fig. 2. Hydrogen bond descriptor plots. The left y-axis on each subplot corresponds to the histograms. The right y-axis on each subplot corresponds to the line graph. See text for a full explanation.

Table 2

Harmonic frequencies in cm^{-1} for the species shown. Numbers enclosed in parenthesis are IR intensities (km/mol). Third number from left is the frequency shift from isolated H_2O or H_2SO_4 . The symbols ν_{wn} and ν_n indicate the isolated molecule ($w = \text{H}_2\text{O}$, $s = \text{H}_2\text{SO}_4$) and mode, n (see the H_2O and H_2SO_4 columns below), the shift is calculated from. The two letters in brackets indicate the positional location (in the dimer in Fig. 1) of the molecule in question: for a H_2SO_4 intramolecular vibrational mode $rs =$ right sulfuric acid, $ls =$ left sulfuric acid. For a H_2O intramolecular vibrational mode, first letter indicates: left, center or right, second letter indicates: top or bottom. Intermolecular stretch modes are indicated by groups of H_2O : left, center, right and both for H_2SO_4

H_2O	H_2SO_4	$(\text{H}_2\text{SO}_4)_2$	$(\text{H}_2\text{SO}_4)_2\text{-H}_2\text{O}$	$(\text{H}_2\text{SO}_4)_2\text{-2H}_2\text{O}$	$(\text{H}_2\text{SO}_4)_2\text{-3H}_2\text{O}$	$(\text{H}_2\text{SO}_4)_2\text{-4H}_2\text{O}$	$(\text{H}_2\text{SO}_4)_2\text{-5H}_2\text{O}$	$(\text{H}_2\text{SO}_4)_2\text{-6H}_2\text{O}$
$\nu_w1 = 3923(62)$	$\nu_s1 = 3773(50)$	3768(75)-1, ν_s2	3862(129)-61, ν_w1	3866(98)-57, $\nu_w1[\text{ct}]$	3881(115)-42, $\nu_w1[\text{lw}]$	3882(100)-41, $\nu_w1[\text{rw}]$	3881(109)-42, $\nu_w1[\text{rw}]$	3881(107)-42, $\nu_w1[\text{rt}]$
$\nu_w2 = 3822(7)$	$\nu_s2 = 3768(202)$	3767(193)-1, ν_s2	3774(126)1, $\nu_s1[\text{ls}]$	3848(109)-75, $\nu_w1[\text{cb}]$	3864(96)-59, $\nu_w1[\text{ct}]$	3881(144)-42, $\nu_w1[\text{lw}]$	3881(118)-42, $\nu_w1[\text{lt}]$	3879(105)-44, $\nu_w1[\text{lt}]$
$\nu_w3 = 1640(71)$	$\nu_s3 = 1437(297)$	3310(2865)-463, ν_s1	3770(133)-3, $\nu_s1[\text{rs}]$	3774(89)1, $\nu_s1[\text{ls}]$	3849(103)-74, $\nu_w1[\text{cb}]$	3864(92)-59, $\nu_w1[\text{ct}]$	3869(90)-54, $\nu_w1[\text{lb}]$	3870(86)-53, $\nu_w1[\text{lb}]$
	$\nu_s4 = 1186(67)$	3235(10)-538, ν_s1	3601(725)-221, ν_w2	3773(153)0, $\nu_s1[\text{rs}]$	3775(118)2, $\nu_s1[\text{rs}]$	3860(102)-63, $\nu_w1[\text{cb}]$	3867(94)-54, $\nu_w1[\text{ct}]$	3870(92)-53, $\nu_w1[\text{rb}]$
	1185(87)	1431(88)-5, ν_s3	3276(1702)-493, $\nu_s2[\text{rs}]$	3582(1057)-240, $\nu_w2[\text{cb}]$	3745(82)-77, $\nu_w2[\text{lw}]$	3740(86)-82, $\nu_w2[\text{rw}]$	3866(90)-56, $\nu_w1[\text{cb}]$	3868(95)-55, $\nu_w1[\text{ct}]$
	530(20)	1406(69)1-30, ν_s3	2687(2015)-1082, $\nu_s2[\text{ls}]$	3559(449)-263, $\nu_w2[\text{ct}]$	3577(1001)-245, $\nu_w2[\text{ct}]$	3738(104)-84, $\nu_w2[\text{lw}]$	3738(96)-84, $\nu_w2[\text{rw}]$	3867(88)-56, $\nu_w1[\text{cb}]$
	831(333)	1305(5)	1675(38)35, ν_w3	2710(3187)-1059, $\nu_s2[\text{rs}]$	3551(471)-271, $\nu_w2[\text{cb}]$	3561(1360)-261, $\nu_w2[\text{cb}]$	3644(470)-178, $\nu_w2[\text{lt}]$	3647(384)-175, $\nu_w2[\text{lt}]$
	775(112)	1300(139)	1423(34)-13, $\nu_s3[\text{ls}]$	2565(1600)-1204, $\nu_s2[\text{ls}]$	3186(1282)-587, $\nu_s1[\text{ls}]$	3547(174)-275, $\nu_w2[\text{ct}]$	3553(1324)-269, $\nu_w2[\text{ct}]$	3644(535)-178, $\nu_w2[\text{rt}]$
	530(20)	1196(145)	1409(445)	1672(65)32, $\nu_w3[\text{ct}]$	2792(2812)-977, $\nu_s2[\text{ls}]$	3192(1058)-581, $\nu_s1[\text{ls}]$	3534(398)-288, $\nu_w2[\text{cb}]$	3548(161)1-275, $\nu_w2[\text{ct}]$
	519(37)	1187(61)	1348(357)	1670(113)30, $\nu_w3[\text{cb}]$	2529(2076)-1240, $\nu_s2[\text{rs}]$	3183(1552)-590, $\nu_s1[\text{rs}]$	3382(737)-440, $\nu_w2[\text{lb}]$	3533(226)-289, $\nu_w2[\text{cb}]$
	478(42)	1163(235)	1284(76)	1478(114)42, $\nu_s3[\text{ls}]$	1671(68)31, $\nu_w3[\text{both}]$	2742(4422)-1027, $\nu_s2[\text{both}]$	3192(1298)-581, $\nu_s1[\text{rs}]$	3384(881)-438, $\nu_w2[\text{rb}]$
	424(19)	1133(151)	1194(144)	1446(137)10, $\nu_s3[\text{rs}]$	1670(11)30, $\nu_w3[\text{both}]$	2681(580)-1088, $\nu_s2[\text{both}]$	2834(2301)-939, $\nu_s1[\text{ls}]$	3382(597)-440, $\nu_w2[\text{lb}]$
	356(3)	896(294)	1188(12)	1350(297)	1645(56)5, $\nu_w3[\text{lw}]$	1673(53)33, $\nu_w3[\text{ct}]$	2735(2662)-1034, $\nu_s2[\text{ls}]$	2827(2157)-946, $\nu_s1[\text{both}]$
	332(57)	886(256)	1165(173)	1344(264)	1485(113)49, $\nu_s3[\text{rs}]$	1666(29)26, $\nu_w3[\text{cb}]$	2722(2372)-1047, $\nu_s2[\text{rs}]$	2791(1031)-982, $\nu_s1[\text{both}]$
	250(93)	807(234)	1148(312)	1188(128)	1448(74)4, $\nu_w3[\text{lw}]$	1645(74)4, $\nu_w3[\text{lw}]$	1679(17)39, $\nu_w3[\text{left}]$	2738(415)-1031, $\nu_s2[\text{both}]$
		794(45)	1080(66)	1187(14)	1404(91)	1641(64)1, $\nu_w3[\text{rw}]$	1674(57)34, $\nu_w3[\text{cb}]$	2733(5885)-1036, $\nu_s1[\text{both}]$
		770(11)	913(290)	1162(459)	1345(289)	1469(186)33, $\nu_s3[\text{ls}]$	1669(19)29, $\nu_w3[\text{ct}]$	1678(16)38, $\nu_w3[\text{right}]$
		720(56)	888(250)	1155(92)	1291(266)	1464(121)28, $\nu_s3[\text{rs}]$	1650(74)10, $\nu_w3[\text{left}]$	1678(24)38, $\nu_w3[\text{left}]$
		549(80)	818(161)	1095(49)	1187(76)	1432(96)	1644(74)4, $\nu_w3[\text{rw}]$	1672(56)32, $\nu_w3[\text{center}]$
		538(11)	796(150)	1069(128)	1161(404)	1421(62)	1479(96)43, $\nu_s3[\text{ls}]$	1669(14)29, $\nu_w3[\text{center}]$
		528(23)	768(12)	919(301)	1151(120)	1291(270)	1466(185)30, $\nu_s3[\text{rs}]$	1652(68)11, $\nu_w3[\text{left}]$
		524(16)	681(131)	913(240)	1101(77)	1282(381)	1440(63)	1650(79)9, $\nu_w3[\text{right}]$
		512(18)	541(8)	809(144)	1023(122)	1153(323)	1419(75)	1479(88)42, $\nu_s3[\text{ls}]$
		492(12)	535(37)	792(173)	924(349)	1143(138)	1292(219)	1475(143)39, $\nu_s3[\text{rs}]$
		420(8)	531(35)	696(68)	914(283)	1056(28)	1284(605)	1443(74)
		417(45)	528(23)	665(123)	861(58)	1030(179)	1154(276)	1437(44)
		369(5)	515(40)	559(47)	837(71)	931(324)	1147(210)	1294(363)
		367(0)	501(4)	544(21)	808(165)	926(409)	1046(35)	1283(580)
		264(140)	442(52)	535(76)	689(49)	844(67)	1013(151)	1154(271)
		263(0)	413(85)	528(21)	679(133)	837(88)	991(158)	1147(246)
		184(55)	408(4)	515(27)	562(72)	817(80)	943(331)	1042(36)
		140(0)	396(14)	513(41)	550(8)	814(74)	930(346)	1009(152)
		118(1)	377(3)	495(50)	548(122)	697(63)	902(73)	989(208)
		51(4)	292(80)	472(14)	539(47)	668(102)	858(47)	984(72)
		41(1)	270(18)	423(58)	528(28)	565(77)	836(89)	943(300)
		22(1)	259(58)	421(17)	524(160)	562(94)	811(79)	935(352)
			229(83)	391(44)	515(102)	555(142)	696(69)	919(107)
			164(28)	380(3)	500(57)	551(2)	669(87)	894(78)
			151(16)	360(64)	476(32)	540(44)	634(158)	859(43)
			89(7)	292(108)	424(17)	534(26)	566(6)	857(36)
			80(3)	280(23)	422(11)	516(117)	564(83)	697(71)
			51(2)	272(11)	392(47)	515(68)	555(108)	672(95)
			32(2)	249(60)	378(33)	484(35)	553(39)	633(182)
			26(1)	238(71)	366(46)	483(36)	543(31)	630(148)
			18(3)	171(56)	331(58)	419(18)	538(27)	567(13)
				154(2)	309(106)	400(86)	515(123)	561(15)

Table 2 (continued)

H ₂ O	H ₂ SO ₄	(H ₂ SO ₄) ₂	(H ₂ SO ₄) ₂ ·H ₂ O	(H ₂ SO ₄) ₂ ·2H ₂ O	(H ₂ SO ₄) ₂ ·3H ₂ O	(H ₂ SO ₄) ₂ ·4H ₂ O	(H ₂ SO ₄) ₂ ·5H ₂ O	(H ₂ SO ₄) ₂ ·6H ₂ O
				90(14)	279(46)	386(15)	501(130)	554(95)
				87(7)	269(16)	375(32)	487(33)	549(96)
				56(1)	240(67)	357(203)	479(18)	546(31)
				44(2)	233(17)	350(76)	420(17)	543(19)
				39()	225(61)	343(41)	408(85)	509(67)
				33(2)	168(54)	311(84)	399(11)	501(101)
				20(2)	151(3)	277(18)	375(28)	488(30)
				12(2)	123(46)	266(34)	372(7)	479(22)
					90(8)	234(79)	347(109)	433(37)
					86(12)	230(13)	337(111)	408(84)
					60(1)	224(34)	320(58)	398(9)
					46(3)	221(55)	297(137)	385(18)
					44()	165(86)	286(7)	373(5)
					36(1)	150(1)	275(7)	364(5)
					26(2)	131(41)	265(44)	337(85)
					23(2)	125(37)	250(123)	332(100)
					16(1)	84(3)	233(35)	325(97)
						80(11)	226(7)	313(125)
						59(5)	222(53)	288(50)
						52()	181(89)	286(15)
						38(1)	157(29)	272(16)
						34(1)	140(3)	263(119)
						24(1)	129(45)	254(68)
						21(4)	111(1)	252(90)
						17(3)	85()	232(23)
						8(1)	81(13)	226(3)
							59(3)	181(95)
							52(2)	165(40)
							36(1)	155(12)
							31(4)	141(2)
							26(1)	110(1)
							22(1)	109(3)
							16(1)	87(7)
							14(2)	81(7)
							10(2)	63(1)
								56(2)
								36(1)
								34()
								26(2)
								24(2)
								20(2)
								18(1)
								15(1)
								7(1)

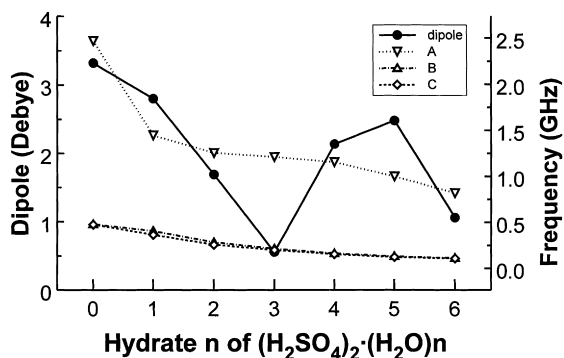


Fig. 3. Rotational constants and dipole moments for each dimer hydrate studied.

intermolecular length (in Å) of the acceptor oxygen to hydrogen distance (OH···O). Donor length will show the intramolecular distance (in Å) between the donor's hydrogen and oxygen (O–H). The supplement angle value will show the deviation from linearity between the three atoms: $180^\circ - \angle O-H \cdots O$. A shorthand notation is sometimes used for representing the formula $(H_2SO_4)_2 \cdot nH_2O$ with DM_n where $n = 0-6$. It should be mentioned that due to the very large size of these systems at this level of theory, one does not have the luxury of looking at other possible conformers. We again stress that a fairly good method for locating the best candidate for a global minimum is to maximize the amount of hydrogen bonds that can form between water and sulfuric acid. Structures for $(H_2SO_4)_2 \cdot nH_2O$ ($n = 0-6$) are shown in Fig. 1. Fig. 2 shows a general trend of the HBDs of each molecule. Column A of Fig. 2 shows the donor's intermolecular hydrogen bond distance with increasing hydrate size, column B of Fig. 2 shows the intramolecular distance (in Å) between the donor's hydrogen and oxygen and column C shows the supplement angle of the hydrogen bond. Each row of Fig. 2 shows the number of different types of hydrogen bonds present in this system. There are four different types of hydrogen bonds in this system:

1. Sulfuric acid –OH to water
2. Sulfuric acid π -d O to water
3. Water to water hydrogen bonds
4. Sulfuric acid to sulfuric acid hydrogen bonds

Only the first three are plotted, the fourth only occurs in DM0 and DM1 and since it is not involved in the

chemical mechanism describing ultrafine aerosol measurements, it is not shown in this figure. In addition, each subplot has on its right y axis the distance between the two oxygens involved in the hydrogen bonding, $R(O-O)$. Figs 3 and 4 show the rotational constants and dipoles for each hydrate respectively. Table 2 contains the harmonic frequencies and intensities computed for the species studied. In addition, Table 2 contains all intramolecular and some intermolecular (where appropriate) frequency shifts from the isolated parent molecules. The frequency shifts are primarily calculated from stretch and bend modes involving –OH which are involved in hydrogen bonding.

3.1.1. $(H_2SO_4)_2$

$(H_2SO_4)_2$ most likely plays a small role in the atmosphere because the concentration of water is many orders of magnitude greater than H_2SO_4 . Consequently the probability of finding free $(H_2SO_4)_2$ will be practically zero. $(H_2SO_4)_2$ has been studied in the past at a few different conformations [35]. The C_2 conformation of the molecule has not been previously studied. The structure for $(H_2SO_4)_2$ (DM0) is shown in Fig. 1. DM0 has two fairly strong type 4 hydrogen bonds with HBD of (1.68, 1.00, 3.2) and a C_2 symmetry. Certainly there are other possible structures, but it is unlikely they can form the similar two strong hydrogen bonds present in DM0. DM0 has only one type of hydrogen bond and that is between two sulfuric acids and so it is consequently not shown on Fig. 2. Most of the atoms in DM0 are arranged around the center in a ring-like formation causing it to have two small very similar rotational constants and a larger rotational constant as shown in Fig. 3. DM0 has the largest dipole moment of the dimer hydrates. This can be explained by the partial alignment of the external unbonded π -d –S=O bonds. Consequently, the –SOH stretch causes a very large change in dipole resulting in a very intense peak at 3310 cm^{-1} as shown in Table 2. The two type 4 hydrogen bonds that form in this system red shift the asymmetric –SOH stretch of both H_2SO_4 's from 3768 to 3310 cm^{-1} and 3235 cm^{-1} .

3.1.2. $(H_2SO_4)_2 \cdot H_2O$

The addition of a water molecule “inside” DM1 cause considerable distortion of the geometry of the

Table 3
Thermodynamic DFT Results at 298 K and 1 atm

	ΔE (kcal/mol)	ΔH (kcal/mol)	ΔS (kcal/(mol K))	ΔG (kcal/mol)	K_p
Addition by H_2SO_4					
$2H_2SO_4 \rightleftharpoons (H_2SO_4)_2$	-12.6	-13.2	-35.6	-2.5	72.9
$H_2SO_4 \cdot H_2O + H_2SO_4 \rightleftharpoons (H_2SO_4)_2 \cdot H_2O$	-11.1	-11.7	-33.3	-1.7	18.2
$H_2SO_4 \cdot 2H_2O + H_2SO_4 \rightleftharpoons (H_2SO_4)_2 \cdot 2H_2O$	-10.9	-11.5	-32.4	-1.9	22.8
$H_2SO_4 \cdot 3H_2O + H_2SO_4 \rightleftharpoons (H_2SO_4)_2 \cdot 3H_2O$	-10.6	-11.2	-33.8	-1.2	7.1
$H_2SO_4 \cdot 4H_2O + H_2SO_4 \rightleftharpoons (H_2SO_4)_2 \cdot 4H_2O$	-10.2	-10.8	-29.3	-2.0	31.7
$H_2SO_4 \cdot 5H_2O + H_2SO_4 \rightleftharpoons (H_2SO_4)_2 \cdot 5H_2O$	-13.9	-14.5	-31.3	-5.1	5906.2
$H_2SO_4 \cdot 6H_2O + H_2SO_4 \rightleftharpoons (H_2SO_4)_2 \cdot 6H_2O$	-16.2	-16.8	-35.2	-6.3	40809.8
Addition by water					
$(H_2SO_4)_2 + H_2O \rightleftharpoons (H_2SO_4)_2 \cdot H_2O$	-7.6	-8.2	-28.2	0.2	0.7
$(H_2SO_4)_2 \cdot H_2O + H_2O \rightleftharpoons (H_2SO_4)_2 \cdot 2H_2O$	-8.5	-9.1	-29.7	-0.3	1.6
$(H_2SO_4)_2 \cdot 2H_2O + H_2O \rightleftharpoons (H_2SO_4)_2 \cdot 3H_2O$	-9.0	-9.6	-32.7	0.2	0.8
$(H_2SO_4)_2 \cdot 3H_2O + H_2O \rightleftharpoons (H_2SO_4)_2 \cdot 4H_2O$	-8.3	-8.9	-28.1	-0.5	2.4
$(H_2SO_4)_2 \cdot 4H_2O + H_2O \rightleftharpoons (H_2SO_4)_2 \cdot 5H_2O$	-9.2	-9.8	-31.6	-0.3	1.7
$(H_2SO_4)_2 \cdot 5H_2O + H_2O \rightleftharpoons (H_2SO_4)_2 \cdot 6H_2O$	-9.7	-10.2	-32.5	-0.5	2.5
Addition by $(H_2SO_4)_n \cdot mH_2O$					
$2H_2SO_4 \cdot H_2O \rightleftharpoons (H_2SO_4)_2 \cdot 2H_2O$	-10.5	-11.1	-32.5	-1.4	10.1
$H_2SO_4 \cdot H_2O + H_2SO_4 \cdot 2H_2O \rightleftharpoons (H_2SO_4)_2 \cdot 3H_2O$	-10.8	-11.4	-34.5	-1.1	6.1
$H_2SO_4 \cdot 2H_2O + H_2SO_4 \cdot 2H_2O \rightleftharpoons (H_2SO_4)_2 \cdot 4H_2O$	-10.4	-11.0	-32.0	-1.5	12.0
$H_2SO_4 \cdot 2H_2O + H_2SO_4 \cdot 3H_2O \rightleftharpoons (H_2SO_4)_2 \cdot 5H_2O$	-10.3	-10.9	-32.4	-1.3	8.6
$2H_2SO_4 \cdot 3H_2O \rightleftharpoons (H_2SO_4)_2 \cdot 6H_2O$	-10.7	-11.3	-33.6	-1.3	8.9

molecule. The C_2 symmetry is lost as well as the alignment of the unbonded π -d $-S=O$ bonds. This causes a noticeable drop in dipole. Also, the additional water molecule causes an elongation of the molecule in its smallest moment of inertia which results in a drop in rotational constant C . However, the additional water molecule forms an additional hydrogen bond of type 2. The type 1 hydrogen bond causes a large noticeable red shift in the donor's $-SOH$ stretch from 3768 to 2687 cm^{-1} which in turn blue shifts the added water's scissor mode from 1640 to 1675 cm^{-1} . The water is also a hydrogen bond donor to one of the π -d oxygens on sulfuric acid which causes its symmetric and asymmetric $-OH$ stretches to red shift from 3923 to 3862 cm^{-1} and from 3822 to 3601 cm^{-1} .

3.1.3. $(H_2SO_4)_2 \cdot 2H_2O$

There is a slight geometric distortion in DM2 caused by the additional water molecule. This slight distortion causes only a slight increment in its smallest moment of inertia resulting in a decrease of rotational constant C . There is another considerable drop in its dipole reflecting the opposite orientation of the added

water's dipole towards the two sulfur acid's dipoles. The last type 4 hydrogen bond present in DM1 is replaced by a type 1 and type 2 hydrogen bond. The two $-SOH$ stretches originally at 3768 cm^{-1} are now significantly red shifted to 2565 and 2710 cm^{-1} accompanied by the usual blue shifts of the water modes indicates a large shift of electron density into the new type 1 hydrogen bonds. This is indicative of very large transfers of electron density into these bonds.

3.1.4. $(H_2SO_4)_2 \cdot 3H_2O$

DM3 contains three water molecules. There are two water molecules that are held in place by two type 1 and two type 2 hydrogen bonds between the two sulfuric acids and the third water molecules is on the "outside" of the dimer hydrogen bonded to an $-SOH$ as shown in Fig. 1. Fig. 2 shows that the external water molecule has a fairly longer type 1 hydrogen bond which is primarily caused by an increase in the $R(O-O)$ supplement angle due to ring strain which results in smaller overlap of the two oxygen and hydrogen atom MOs involved in the hydrogen bond formation. The free $-SOH$ is now a donor in a fairly

Table 4

ΔH , ΔG (in kcal/mol) and ΔS for the reactions of $\text{H}_2\text{SO}_4 \cdot n\text{H}_2\text{O} + \text{H}_2\text{SO}_4 \rightleftharpoons (\text{H}_2\text{SO}_4)_2 \cdot n\text{H}_2\text{O}$ ($n = 0-6$) at the temperatures indicated

	273 K				248 K				223 K				198 K				173 K			
	ΔH	ΔS	ΔG	K_p	ΔH	ΔS	ΔG	K_p	ΔH	ΔS	ΔG	K_p	ΔH	ΔS	ΔG	K_p	ΔH	ΔS	ΔG	K_p
$(\text{H}_2\text{SO}_4)_2$	-13.2	-35.7	-3.4	557.2	-13.2	-35.8	-4.3	6468.9	-13.2	-35.9	-5.2	1.3×10^5	-13.3	-36.1	-6.1	5.7×10^6	-13.3	-36.2	-7.0	7.4×10^8
$(\text{H}_2\text{SO}_4)_2 \cdot \text{H}_2\text{O}$	-11.7	-33.4	-2.6	110.3	-11.7	-33.6	-3.4	969.1	-11.8	-33.7	-4.2	1.4×10^4	-11.8	-33.8	-5.1	4.0×10^5	-11.8	-34.0	-5.9	3.0×10^7
$(\text{H}_2\text{SO}_4)_2 \cdot 2\text{H}_2\text{O}$	-11.5	-32.5	-2.7	134.8	-11.6	-32.6	-3.5	1147.9	-11.6	-32.7	-4.3	1.6×10^4	-11.6	-32.8	-5.1	4.3×10^5	-11.6	-32.9	-5.9	3.0×10^7
$(\text{H}_2\text{SO}_4)_2 \cdot 3\text{H}_2\text{O}$	-11.3	-33.9	-2.0	40.5	-11.3	-34.0	-2.9	328.5	-11.3	-34.2	-3.7	4.3×10^3	-11.4	-34.3	-4.6	1.1×10^5	-11.4	-34.5	-5.4	7.0×10^6
$(\text{H}_2\text{SO}_4)_2 \cdot 4\text{H}_2\text{O}$	-10.8	-29.5	-2.8	168.0	-10.9	-29.8	-3.5	1266.8	-11.0	-30.0	-4.3	1.5×10^4	-11.0	-30.3	-5.0	3.5×10^5	-11.1	-30.6	-5.8	2.0×10^7
$(\text{H}_2\text{SO}_4)_2 \cdot 5\text{H}_2\text{O}$	-14.5	-31.5	-5.9	55220.1	-14.6	-31.6	-6.7	822 770	-14.6	-31.8	-7.5	2.3×10^7	-14.7	-32.0	-8.3	1.4×10^9	-14.7	-32.2	-9.1	3.1×10^{11}
$(\text{H}_2\text{SO}_4)_2 \cdot 6\text{H}_2\text{O}$	-16.8	-35.2	-7.2	544254	-16.8	-35.3	-8.1	12 329 535	-16.8	-35.4	-8.9	5.6×10^8	-16.9	-35.5	-9.8	6.8×10^{10}	-16.9	-35.6	-10.7	3.3×10^{13}

Table 5

 ΔH , ΔG (in kcal/mol) and ΔS for the reactions of $(\text{H}_2\text{SO}_4)_2 \cdot n\text{H}_2\text{O} + \text{H}_2\text{O} \Leftrightarrow (\text{H}_2\text{SO}_4)_2 \cdot (n + 1)\text{H}_2\text{O}$ ($n = 0-5$) at the temperatures indicated

	273 K				248 K				223 K				198 K				173 K			
	ΔH	ΔS	ΔG	K_p	ΔH	ΔS	ΔG	K_p	ΔH	ΔS	ΔG	K_p	ΔH	ΔS	ΔG	K_p	ΔH	ΔS	ΔG	K_p
$(\text{H}_2\text{SO}_4)_2 \cdot \text{H}_2\text{O}$	-8.2	-28.3	-0.5	2.5	-8.2	-28.4	-1.2	11.5	-8.3	-28.4	-1.9	7.5×10	-8.3	-28.4	-2.6	7.8×10^2	-8.3	-28.4	-3.3	1.6×10^4
$(\text{H}_2\text{SO}_4)_2 \cdot 2\text{H}_2\text{O}$	-9.1	-29.8	-1.0	6.4	-9.1	-29.8	-1.8	34.7	-9.1	-29.8	-2.5	2.8×10^2	-9.1	-29.7	-3.2	3.7×10^3	-9.1	-29.5	-4.0	1.0×10^5
$(\text{H}_2\text{SO}_4)_2 \cdot 3\text{H}_2\text{O}$	-9.6	-32.7	-0.7	3.3	-9.6	-32.8	-1.5	19.8	-9.6	-32.8	-2.3	1.7×10^2	-9.6	-32.7	-3.1	2.7×10^3	-9.6	-32.6	-3.9	9.0×10^4
$(\text{H}_2\text{SO}_4)_2 \cdot 4\text{H}_2\text{O}$	-8.9	-28.2	-1.2	9.6	-9.0	-28.3	-1.9	50.8	-9.0	-28.3	-2.6	3.9×10^2	-9.0	-28.3	-3.4	5.0×10^3	-8.9	-28.2	-4.1	1.3×10^5
$(\text{H}_2\text{SO}_4)_2 \cdot 5\text{H}_2\text{O}$	-9.8	-31.7	-1.1	7.8	-9.8	-31.7	-1.9	47.8	-9.8	-31.6	-2.7	4.4×10^2	-9.7	-31.5	-3.5	7.0×10^3	-9.7	-31.3	-4.3	2.5×10^5
$(\text{H}_2\text{SO}_4)_2 \cdot 6\text{H}_2\text{O}$	-10.2	-32.5	-1.4	12.3	-10.2	-32.5	-2.2	82.1	-10.2	-32.4	-3.0	8.4×10^2	-10.2	-32.3	-3.8	1.5×10^4	-10.2	-32.1	-4.6	6.3×10^5

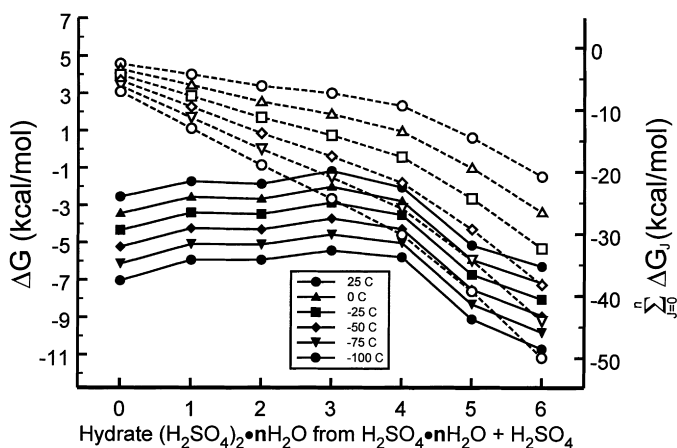


Fig. 4. Successive free energy plot (filled symbols, left axis) and cumulative free energy plot (open symbols, right axis) of the reactions of $\text{H}_2\text{SO}_4 \cdot n\text{H}_2\text{O} + \text{H}_2\text{SO}_4 \rightleftharpoons \text{H}_2\text{SO}_4 \cdot (n+1)\text{H}_2\text{O}$, $n = 0-6$.

strong hydrogen bond as shown by the red shift it undergoes from 3773 in DM2 to 3186 cm^{-1} . Once again the strongest bonds of type 1 still show the largest red shift of frequencies from 3768 to 2792 and 2529 cm^{-1} . There is extensive delocalization of the $-\text{OH}$ stretch modes, 1670 and 1671 cm^{-1} , on the center water molecules. Also, there is no major change in the moments of inertia for this molecule as shown by the almost zero change in the rotational constants. The dipole for DM3 has decreased again. This is possibly due to the dipole of the external water molecule oriented in a slightly opposite direction with respect to the two sulfuric acids.

3.1.5. $(\text{H}_2\text{SO}_4)_2 \cdot 4\text{H}_2\text{O}$

There are four water molecules present in DM4. Two water molecules present between the two sulfuric acid molecules as before and two water molecules that are hydrogen bonded on the “left” and “right” sides of the dimer as shown in Fig. 1. Fig. 2 shows that the $R(\text{O}-\text{O})$ distance for type 2 hydrogens has undergone a slight contraction. The two external water molecules present in DM4 also have a longer $R(\text{O}-\text{O})$ type 2 hydrogen bond compared to the two internal type 2 hydrogen bonds as shown in Fig. 2. Once again this is possibly due to ring strain causing the larger supplement angle. Also, there is no major change in the moments of inertia for this molecule as shown by the almost zero change in the rotational constants. The new type 2 hydrogen bond is also

strong and similar to the one in DM3. In addition to the previous red shifts in frequencies, Table 2 shows that this type 2 hydrogen bond also causes a fairly large red shift in the remaining $-\text{SOH}$ frequency from 3773 to 3183 cm^{-1} . Also, there is extensive delocalization of the 2742 and 2681 cm^{-1} stretching modes of H_2SO_4 .

3.1.6. $(\text{H}_2\text{SO}_4)_2 \cdot 5\text{H}_2\text{O}$

The additional fifth water molecule to DM4 causes some physical changes to happen in DM5. The additional water molecule’s dipole is slightly aligned with DM4 causing the dipole to increase slightly. Also, there is a ring expansion which causes much less ring strain resulting in a strengthening of the type 1 hydrogen bond present on the “left” side of the molecule as its HBD decreases from (1.70, 1.00, 15.2) in DM4 to (1.55, 1.02, 2.7) in DM5. Fig. 3 shows the continuation of the decrease in rotational constants as the amount of water molecules is increased from 4 to 5. The extensive delocalization of the stretching modes involved in hydrogen bond formation is even more apparent in this molecule. Now all the stretching frequencies of sulfuric acid all show large red shifts which is indicative of strong hydrogen bond formation.

3.1.7. $(\text{H}_2\text{SO}_4)_2 \cdot 6\text{H}_2\text{O}$

Sulfuric acid with six water molecules, DM6, has been shown in our previous paper and is included in

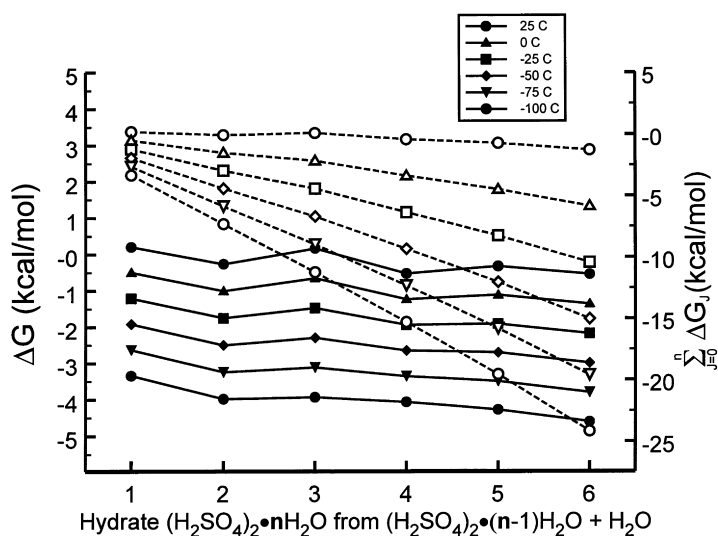


Fig. 5. Successive free energy plot (filled symbols, left axis) and cumulative free energy plot (open symbols, right axis) of the reactions of $(\text{H}_2\text{SO}_4)_n\text{H}_2\text{O} + \text{H}_2\text{O} \rightleftharpoons (\text{H}_2\text{SO}_4)_2 \cdot (n+1)\text{H}_2\text{O}$, $n = 0-5$.

this paper for a more thorough analysis and to compare it with the other hydrated dimers. An additional water molecule is added on the “right” side of the molecule. It is possible to add a water molecule on the “left” side resulting in two type 2 hydrogen bonds not the additional type 1 and type 2 hydrogen bond. It was shown that water–water hydrogen bonds as not as exothermic as water–sulfuric acid hydrogen bonds resulting in a larger enthalpy for that system [24], so

consequently a conformer of DM6 with three waters on one side was not investigated. One can see that the strong interacting type 1 hydrogen bonds are overall the smallest in this system due to the complete elimination of ring strain as shown in Figs. 1 and 2. The large decrease in dipole is primarily due to the opposite alignment of the additional water molecule’s dipole. Table 2 shows one enormous peak at 2733 cm^{-1} . This frequency corresponds to a very

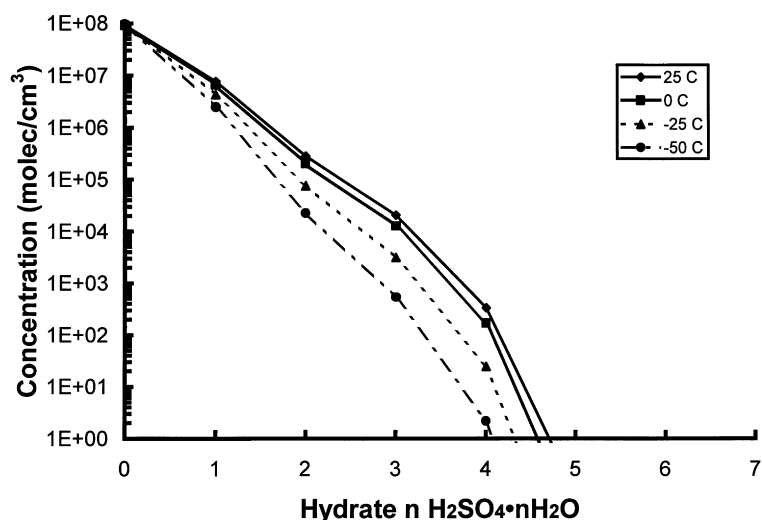


Fig. 6. Equilibrium concentrations of $\text{H}_2\text{SO}_4 \cdot n\text{H}_2\text{O}$ ($n = 0-12$) at four different temperatures (see text for full details).

delocalized –SOH stretch mode. This very delocalized stretch mode significantly alters the electron density and causes a large change in the dipole for that mode resulting in a very intense peak. As before, the stretching frequencies of sulfuric acid all show large red shifts, which is indicative of strong hydrogen bond formation in this molecule.

4. Hydrate energetics

The electronic energy and the zero-point vibrational energy are given in Table 1 as well as the thermal energy and entropy at 173, 198, 223, 248, 273 and 298 K for each of the hydrates studied. The electronic energies, thermal energies and entropies for H_2O and $\text{H}_2\text{SO}_4 \cdot n\text{H}_2\text{O}$, $n = 0-6$ used in the dimer hydrate energetics calculation were taken from our previous paper [24]. The temperature range was selected to correspond to the approximate range of temperatures found in the troposphere and stratosphere. Free energies, entropies, enthalpies and internal energies of formation of $(\text{H}_2\text{SO}_4)_2 \cdot n\text{H}_2\text{O}$ from $\text{H}_2\text{SO}_4 \cdot n\text{H}_2\text{O} + \text{H}_2\text{SO}_4$, $(\text{H}_2\text{SO}_4)_2 \cdot (n-1)\text{H}_2\text{O} + \text{H}_2\text{O}$ and selected combinations of $\text{H}_2\text{SO}_4 \cdot n\text{H}_2\text{O} + \text{H}_2\text{SO}_4 \cdot n\text{H}_2\text{O}$ at 298 K and 1 atm are given in Table 3. Free energies, entropies and enthalpies of formation, of $(\text{H}_2\text{SO}_4)_2 \cdot n\text{H}_2\text{O}$ from $(\text{H}_2\text{SO}_4)_2 \cdot (n-1)\text{H}_2\text{O} + \text{H}_2\text{SO}_4$ over the temperatures of 173, 198, 223, 248 and 273 K are given in Table 4. Also, free energies, entropies and enthalpies of formation, of $(\text{H}_2\text{SO}_4)_2 \cdot n\text{H}_2\text{O}$ from $(\text{H}_2\text{SO}_4)_2 \cdot (n-1)\text{H}_2\text{O} + \text{H}_2\text{O}$ over the temperatures of 173, 198, 223, 248, 273 and 298 K are given in Table 5.

Plots of the free energy for the reactions $\text{H}_2\text{SO}_4 \cdot n\text{H}_2\text{O} + \text{H}_2\text{SO}_4 \rightleftharpoons (\text{H}_2\text{SO}_4)_2 \cdot n\text{H}_2\text{O}$ as a function of n are shown in Fig. 4. The free energy is around -2 kcal for the first four hydrate dimers and then subsequent -3 and -4 kcal drops in free energies for dimer hydrates 5 and 6. A possible explanation is that those structures do not have the ring strain that was present in the previous dimer hydrates, as was mentioned in Section 3.1. As the temperature is lowered the $T\Delta S$ term becomes more positive by about 1 kcal/mol per 25°C resulting in lowering of ΔG of about 1 kcal/mol per 25°C .

The cumulative free energy of formation of $(\text{H}_2\text{SO}_4)_2 \cdot n\text{H}_2\text{O}$ from $\text{H}_2\text{SO}_4 \cdot n\text{H}_2\text{O}$ and H_2SO_4 is

shown in Fig. 4, right axis, for each of the hydrates studied. Inspection of Fig. 4 reveals that all the higher hydrates of $(\text{H}_2\text{SO}_4)_2$ linearly decrease the free energy of the system for hydrates 1–4 and even greater release of free energy for hydrates 4 and 5.

There are more thermodynamic routes to form $(\text{H}_2\text{SO}_4)_2 \cdot n\text{H}_2\text{O}$. The dimer hydrates can also form from possible collisions with the sulfuric acid monomer hydrates, but they are not as energetically favorable as the combination reaction of the monomer hydrate and free sulfuric acid as shown in Table 3. In addition, they are less likely to happen since the concentration of free sulfuric acid, at equilibrium, is so much higher than most of the higher monomer hydrates as shown in Fig. 6.

Plots of the free energy for the reactions $(\text{H}_2\text{SO}_4)_2 \cdot (n-1)\text{H}_2\text{O} + \text{H}_2\text{O} \rightleftharpoons (\text{H}_2\text{SO}_4)_2 \cdot n\text{H}_2\text{O}$ as a function of n are shown in Fig. 5. The magnitude of the free energies of the reaction of $(\text{H}_2\text{SO}_4)_2 \cdot (n-1)\text{H}_2\text{O} + \text{H}_2\text{O} \rightleftharpoons (\text{H}_2\text{SO}_4)_2 \cdot n\text{H}_2\text{O}$ are less than those of $\text{H}_2\text{SO}_4 \cdot n\text{H}_2\text{O} + \text{H}_2\text{SO}_4 \rightleftharpoons (\text{H}_2\text{SO}_4)_2 \cdot n\text{H}_2\text{O}$ mainly because the addition of sulfuric acid creates two hydrogen bonds of type 1 and type 2 while the addition of water will only create a single type 1, 2 or 3 hydrogen bond or two hydrogen bonds of type 2 and a weaker type 3. For 25°C all the ΔG 's are around 0 kcal/mol. As the temperature is lowered the $T\Delta S$ term becomes more positive by about 0.75 kcal/mol per 25°C resulting in a lowering of ΔG of about 0.75 kcal/mol per 25°C .

The cumulative free energy of formation of $(\text{H}_2\text{SO}_4)_2 \cdot n\text{H}_2\text{O}$ from $(\text{H}_2\text{SO}_4)_2 \cdot (n-1)\text{H}_2\text{O}$ and H_2O is shown in Fig. 5, right axis, for each of the hydrates studied. Only at 0°C and below is there an overall decrease in free energy in the system.

4.1. Atmospheric implications

As was mentioned in Section 1, there is an abundance of atmospheric sulfate aerosol measurements, which show a sulfuric acid to water ratio of 1:2. Why does this ratio always seem to be around 1:2?

There are a few good reasons for this. The first reason is that the maximum amount of exothermic bonding between water and sulfuric acid is two waters for each sulfuric acid, m , and four waters for the “beginning” and “end” yielding a formula of $2m + 4$ as demonstrated in our previous paper. Since sulfuric

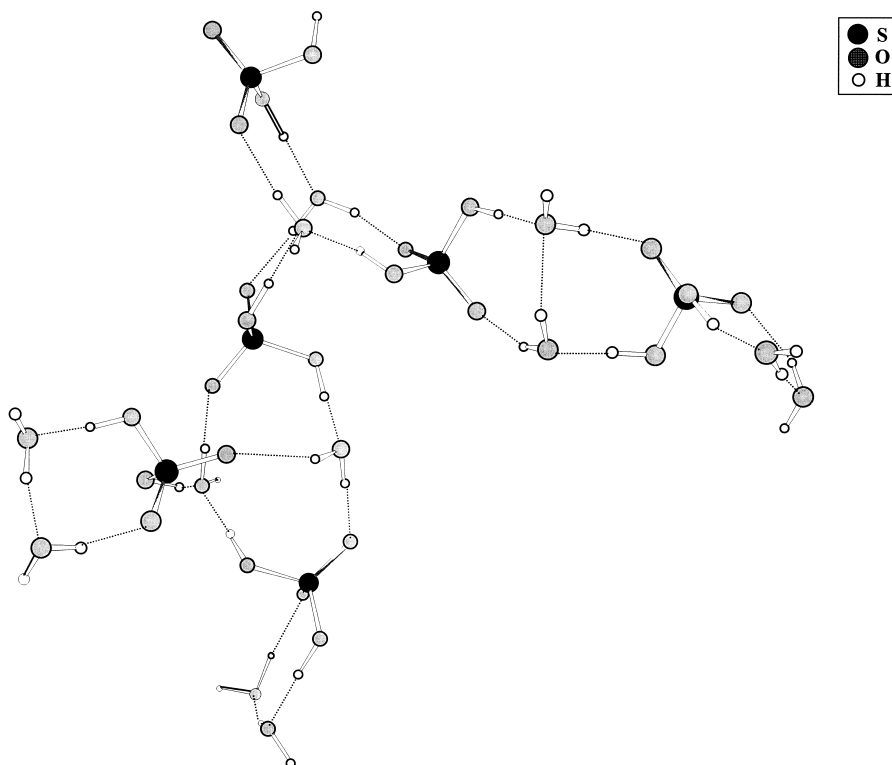


Fig. 7. A possible piece of a larger atmospheric ultrafine aerosol particle. Note the $-(\text{H}_2\text{SO}_4)_2\cdot 2\text{H}_2\text{O}-$ monomer present throughout the structure.

acid can no longer bond with water, adding additional waters will possibly cause more endothermic water–water bonding causing a raising of free energy in the system. This was demonstrated in a previous paper for the $\text{H}_2\text{SO}_4\text{--H}_2\text{O}$ system [24]. A second reason is kinetic.

A kinetic explanation can be devised to explain the 1:2 ratio. This explanation is based on how the two water molecules between each sulfuric acid are connected. Each water molecule is held in place by two strong hydrogen bonds. In Table 3 examining the column of internal energy changes we can assume a crude estimate of the strength of one hydrogen bond at around 8 kcal. The average kinetic energy available to each molecule is $(3/2)RT$, which is around 0.9 kcal/mol at 298 K for all three degrees of freedom. If a water molecule and a growing particle composed of $-(\text{H}_2\text{SO}_4\cdot 2\text{H}_2\text{O})-$ monomers collide, a reasonable assumption is that the translational

energy along the direct line of collision (one degree of freedom for each molecule) will transfer its energy into breaking the hydrogen bond. It is obvious that 0.9 kcal for three degrees of freedom is not enough to rupture a hydrogen bond, but that is for an average kinetic energy. The kinetic energy for this system will have Boltzmann distribution:

$$\frac{n_E}{n_T} = e^{-E/RT} \quad (1)$$

where n_T is the total amount of molecules and n_E the amount of molecules containing a total amount of kinetic energy equal or surpassing E . We can calculate the fraction of molecules present that have $(3/2) \times 8$ kcal/mol of energy which is about 2×10^{-9} . At 1 atm this amounts to 1×10^{10} molecules/cc. By use of collision theory we can get an approximation of the rate of H_2O 's that

Table 6

Reactions for chain growth initialization only. Rate constants are in $\text{cm}^3/(\text{molecule s})$ for bimolecular reactions and $1/\text{s}$ for unimolecular reactions

Reaction no.	Rate constant	Chemical reaction
1	4.27×10^{-10}	$\text{H}_2\text{SO}_4 + \text{H}_2\text{O} \rightarrow \text{H}_2\text{SO}_4 \cdot \text{H}_2\text{O}$
2	9.11×10^8	$\text{H}_2\text{SO}_4 \cdot \text{H}_2\text{O} \rightarrow \text{H}_2\text{SO}_4 + \text{H}_2\text{O}$
3	4.59×10^{-10}	$\text{H}_2\text{SO}_4 \cdot \text{H}_2\text{O} + \text{H}_2\text{O} \rightarrow$ $\text{H}_2\text{SO}_4 \cdot 2(\text{H}_2\text{O})$
4	2.37×10^9	$\text{H}_2\text{SO}_4 \cdot 2(\text{H}_2\text{O}) \rightarrow$ $\text{H}_2\text{SO}_4 \cdot \text{H}_2\text{O} + \text{H}_2\text{O}$
5	4.96×10^{-10}	$\text{H}_2\text{SO}_4 \cdot 2(\text{H}_2\text{O}) + \text{H}_2\text{O} \rightarrow$ $\text{H}_2\text{SO}_4 \cdot 3(\text{H}_2\text{O})$
6	1.20×10^9	$\text{H}_2\text{SO}_4 \cdot 3(\text{H}_2\text{O}) \rightarrow$ $\text{H}_2\text{SO}_4 \cdot 2(\text{H}_2\text{O}) + \text{H}_2\text{O}$
7	5.33×10^{-10}	$\text{H}_2\text{SO}_4 \cdot 3(\text{H}_2\text{O}) + \text{H}_2\text{O} \rightarrow$ $\text{H}_2\text{SO}_4 \cdot 4(\text{H}_2\text{O})$
8	6.17×10^9	$\text{H}_2\text{SO}_4 \cdot 4(\text{H}_2\text{O}) \rightarrow$ $\text{H}_2\text{SO}_4 \cdot 3(\text{H}_2\text{O}) + \text{H}_2\text{O}$
9	5.67×10^{-10}	$\text{H}_2\text{SO}_4 \cdot 4(\text{H}_2\text{O}) + \text{H}_2\text{O} \rightarrow$ $\text{H}_2\text{SO}_4 \cdot 5(\text{H}_2\text{O})$
10	6.42×10^{11}	$\text{H}_2\text{SO}_4 \cdot 5(\text{H}_2\text{O}) \rightarrow$ $\text{H}_2\text{SO}_4 \cdot 4(\text{H}_2\text{O}) + \text{H}_2\text{O}$
11	6.01×10^{-10}	$\text{H}_2\text{SO}_4 \cdot 5(\text{H}_2\text{O}) + \text{H}_2\text{O} \rightarrow$ $\text{H}_2\text{SO}_4 \cdot 6(\text{H}_2\text{O})$
12	1.30×10^{10}	$\text{H}_2\text{SO}_4 \cdot 6(\text{H}_2\text{O}) \rightarrow$ $\text{H}_2\text{SO}_4 \cdot 5(\text{H}_2\text{O}) + \text{H}_2\text{O}$
13	6.34×10^{-10}	$\text{H}_2\text{SO}_4 \cdot 6(\text{H}_2\text{O}) + \text{H}_2\text{O} \rightarrow$ $\text{H}_2\text{SO}_4 \cdot 7(\text{H}_2\text{O})$
14	9.69×10^9	$\text{H}_2\text{SO}_4 \cdot 7(\text{H}_2\text{O}) \rightarrow$ $\text{H}_2\text{SO}_4 \cdot 6(\text{H}_2\text{O}) + \text{H}_2\text{O}$
15	3.64×10^{-10}	$\text{H}_2\text{SO}_4 \cdot 2(\text{H}_2\text{O}) + \text{H}_2\text{SO}_4 \rightarrow$ $(\text{H}_2\text{SO}_4)_2 \cdot 2(\text{H}_2\text{O})$
16	4.30×10^8	$(\text{H}_2\text{SO}_4)_2 \cdot 2(\text{H}_2\text{O}) \rightarrow$ $\text{H}_2\text{SO}_4 \cdot 2(\text{H}_2\text{O}) + \text{H}_2\text{SO}_4$
17	5.44×10^{-10}	$(\text{H}_2\text{SO}_4)_2 \cdot 2(\text{H}_2\text{O}) + \text{H}_2\text{O} \rightarrow$ $(\text{H}_2\text{SO}_4)_2 \cdot 3(\text{H}_2\text{O})$
18	1.93×10^{10}	$(\text{H}_2\text{SO}_4)_2 \cdot 3(\text{H}_2\text{O}) \rightarrow$ $(\text{H}_2\text{SO}_4)_2 \cdot 2(\text{H}_2\text{O}) + \text{H}_2\text{O}$
19	5.62×10^{-10}	$(\text{H}_2\text{SO}_4)_2 \cdot 3(\text{H}_2\text{O}) + \text{H}_2\text{O} \rightarrow$ $(\text{H}_2\text{SO}_4)_2 \cdot 4(\text{H}_2\text{O})$
20	2.00×10^{10}	$(\text{H}_2\text{SO}_4)_2 \cdot 4(\text{H}_2\text{O}) \rightarrow$ $(\text{H}_2\text{SO}_4)_2 \cdot 3(\text{H}_2\text{O}) + \text{H}_2\text{O}$
21	4.18×10^{-10}	$(\text{H}_2\text{SO}_4)_2 \cdot 4(\text{H}_2\text{O}) + \text{H}_2\text{SO}_4 \rightarrow$ $(\text{H}_2\text{SO}_4)_3 \cdot 4(\text{H}_2\text{O})$

are displaced from this growing chain:

$$\frac{d[\text{H}_2\text{O} \text{ lost from chain}]}{dt} = k_{\text{Collision}}[\text{Total Gaseous Molecules}][\text{Chain}] \quad (2)$$

$$[\text{Total Gaseous Molecules}] \approx [\text{N}_2] \approx 1 \times 10^{19} \text{ mole-}$$

Table 7

Final concentrations of sulfuric acid hydrates, dimer and trimer hydrates after 24.5 h of simulation time (see text for full details)

Molecule	Concentration (molecules/ cm^3)
H_2SO_4	9.3×10^7
$\text{H}_2\text{SO}_4 \cdot \text{H}_2\text{O}$	6.7×10^6
$\text{H}_2\text{SO}_4 \cdot (\text{H}_2\text{O})_2$	2.0×10^5
$\text{H}_2\text{SO}_4 \cdot (\text{H}_2\text{O})_3$	12 735
$\text{H}_2\text{SO}_4 \cdot (\text{H}_2\text{O})_4$	169
$\text{H}_2\text{SO}_4 \cdot (\text{H}_2\text{O})_5$	< 1
$\text{H}_2\text{SO}_4 \cdot (\text{H}_2\text{O})_6$	< 1
$\text{H}_2\text{SO}_4 \cdot (\text{H}_2\text{O})_7$	$\ll 1$
$(\text{H}_2\text{SO}_4)_2 \cdot (\text{H}_2\text{O})_2$	$\ll 1$
$(\text{H}_2\text{SO}_4)_2 \cdot (\text{H}_2\text{O})_3$	$\ll 1$
$(\text{H}_2\text{SO}_4)_2 \cdot (\text{H}_2\text{O})_4$	0
$(\text{H}_2\text{SO}_4)_3 \cdot (\text{H}_2\text{O})_4$	0

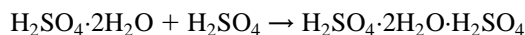
cules/cc, $[\text{Chain}] = 1$ molecule/cc for this example and $k_{\text{Collision}}$:

$$k_{\text{Collision}} = P\pi(r_{\text{N}_2} + r_{\text{H}_2\text{SO}_4 \cdot 2\text{H}_2\text{O}})^2 \sqrt{\frac{8kT}{\pi\mu}} e^{-E_a/RT} \quad (3)$$

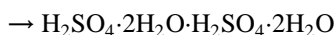
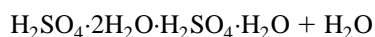
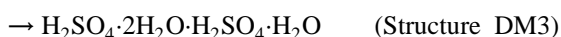
r_{N_2} is the molecular radius of N_2 and is 1.46×10^{-8} cm [36], $r_{\text{H}_2\text{SO}_4 \cdot 2\text{H}_2\text{O}}$ is the molecular radius of $\text{H}_2\text{SO}_4 \cdot 2\text{H}_2\text{O}$ and is approximated from its density [36] of 1.64 g/cm^3 to give 3.36×10^{-10} m, P is unity and $E_a = 0$ since we are interested in only displacing a single hydrogen bond from a collision, μ is the reduced mass and T at 298 K gives $k_{\text{Collision}} \approx 3 \times 10^{-10}$ which yields a disappearance rate of H_2O s from a growing chain at 3×10^9 molecules/ cm^3 s. This disappearance rate will become much larger as the chain grows. If this sulfuric acid–water chain was composed of single hydrogen bonds, it is quite clear that the chain will never grow.

The chain does grow and it is mainly due to the four hydrogen bonds (two on each side of the bonded water molecule) between each sulfuric acid. This allows the growing chain to “heal” itself, for it is very unlikely for two hydrogen bonds to break at the same exact time at the same point in the chain. A ruptured hydrogen bond will reconnect to the sulfuric acid before the other water’s hydrogen bond to the same sulfuric acid is ruptured. With this in mind, a simple kinetic scheme of a growing $-\text{H}_2\text{SO}_4 \cdot 2\text{H}_2\text{O}-$

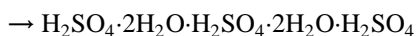
chain can be devised:



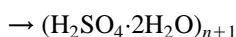
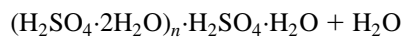
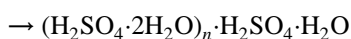
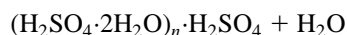
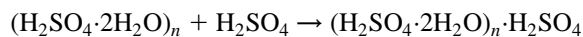
(Structure DM2)



(Structure DM5 minus lone H₂O)



A general scheme:



This chain can branch in any dimension. Inspection of structure DM4 shows that the two middle waters can easily add a sulfuric acid. One water has a free –OH and the other one has a free lone-pair that a sulfuric acid can bind to. This can create twisting three-dimensional structures. A possible very short oligomer is demonstrated in Fig. 7. The question that now remains is there enough free energy for the first few steps to happen?

One can compute an equilibrium distribution of H₂SO₄·*n*H₂O (Fig. 6) if one takes the equilibrium constants from our previous paper and for hydrates above *n* = 7 for H₂SO₄·*n*H₂O assumes the free energy decreases 1 kcal for each H₂O added (very unlikely). The initial concentration of free H₂SO₄ is 10⁸ molecule/cm³ which is about five times higher than most atmospheric measurements [37–41]. A high relative

humidity of 95% is used for all the equilibrium runs. This equilibrium plot shows the maximum concentrations that can happen for this system since we are assuming infinitely fast kinetics and no other reaction pathways. Fig. 6 shows that the hydrates of H₂SO₄·*n*H₂O for *n* ≥ 5 are unimportant in the temperature range of 25 to –50°C. Now the question is it thermodynamically possible to add an additional H₂SO₄ to H₂SO₄·2H₂O? If one takes into account the kinetic mechanism described above and the equilibrium plot, one can assess a maximum concentration of (H₂SO₄)₂·2H₂O that can be formed by formulating a simple equilibrium expression for the formation of (H₂SO₄)₂·2H₂O from H₂SO₄·2H₂O:



$$K_C = \frac{[(\text{H}_2\text{SO}_4)_2 \cdot 2\text{H}_2\text{O}]}{[\text{H}_2\text{SO}_4 \cdot 2\text{H}_2\text{O}][\text{H}_2\text{SO}_4]} \quad (4)$$

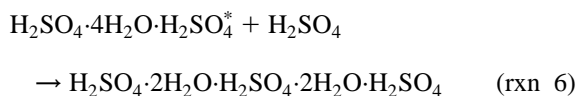
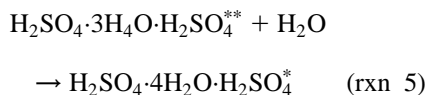
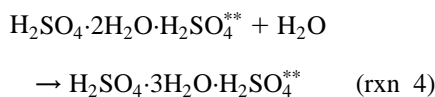
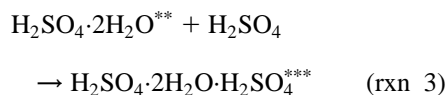
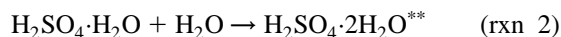
From a Δ*G* of –1.9 kcal/mol (see Table 3) we arrive at a *K*_C = 1 × 10^{–18} at 25°C. Placing the maximum values that H₂SO₄·2H₂O and H₂SO₄ can acquire into Eq. (4) we quickly obtain a value of 1 × 10^{–4} molecule/cc for (H₂SO₄)₂·2H₂O which is the utmost maximum concentration (H₂SO₄)₂·2H₂O can acquire. As mentioned in Section 1, there is a great deal of evidence that shows new particle nucleation can happen at or below 25°C. We can extend the current equilibrium analysis to include kinetic arguments in that the newly formed (H₂SO₄)₂·2H₂O can quickly react with water to very quickly “push” it ahead to form new larger particles before (H₂SO₄)₂·2H₂O can revert back into H₂SO₄·2H₂O and H₂SO₄. We studied this possibility by applying kinetic rate laws to the hydration of H₂SO₄·*n*H₂O, *n* = 0–7 using collision theory (Eq. (3)) to evaluate the forward rate constants and the reverse rate constants from the equilibrium constants and the following expression:

$$K = \frac{k_f}{k_b}$$

For the radius of the hydrates H₂SO₄·*n*H₂O, *n* = 0–7, the specific gravity of the aqueous bulk solution composed of the same %H₂SO₄ as the molecule [42] was used to compute the radius. The same initial concentrations of H₂SO₄ and RH used in the equilibrium model are used here. The chemical kinetic

equations and their respective rate constants are shown in Table 6. Integrating the system with Kintecus VI.78 [43] yields the final concentrations shown in Table 7. Inspection of Table 7 shows that it is quite clear that $(\text{H}_2\text{SO}_4)_2 \cdot 2\text{H}_2\text{O}$ cannot form. Reactions 16, 18 and 20 (Table 6) do not allow the chain to grow. This is contradictory to all the experimental evidence stated in Section 1. An explanation is that the drop in entropy in the reactions is too large. This entropy drop is large enough to cause the reverse rates to have the dominant role at this stage. This system will easily grow if there was a way to bypass these initial reactions. If the system can start at a larger chain size of $-(\text{H}_2\text{SO}_4)_2 \cdot 2\text{H}_2\text{O}-$ where the relative entropy between the products and reactants approach zero, then the $-(\text{H}_2\text{SO}_4)_2 \cdot 2\text{H}_2\text{O}-$ chains in this system will easily grow.

There are essentially four ways for this system to start at a larger chain size of $-(\text{H}_2\text{SO}_4)_2 \cdot 2\text{H}_2\text{O}-$. One way is that there is a third (or more) species present which “helps” the system stabilize clusters of $(\text{H}_2\text{SO}_4)_2 \cdot 2\text{H}_2\text{O}$ and/or increase the concentration of $\text{X} \cdot \text{H}_2\text{SO}_4 \cdot n\text{H}_2\text{O}$ ($n = 2, 4, 6$) where X is some stabilizing species. One possible species is NH_3 . There has been considerable interest in this species for its possible role in new atmospheric particle formation [36,37,39]. We are currently studying this and will present our results in a future paper. A second explanation is that the free energies calculated are too positive. It should be noted that since these clusters are held together by intermolecular hydrogen bonds which are known to be anharmonic [44] there could be some error in the calculated entropies, but recent calculations by Scott and Radom [45] and Sodupe et al. [29] have shown that B3LYP with very large basis sets can reproduce experimental anharmonic low frequencies of covalent and hydrogen bonded compounds. A third reason is that the reactions shown in Table 6 could form excited state products:



Naturally, there are a number of assumptions present in the above reactions. One assumption is that the collision between the bath gas and the excited products do not transfer energy through any “chattering” modes [46]. The stored internal energy is gradually released with reactions 4–6. It should be noted there is no proof for or against this mechanism to initialize the chain growth, and a similar mechanism using excited states of molecules was implied by Jayne et al. [47] to describe gas phase reactions of SO_3 and H_2O . A fourth and final reason is that there are particles formed from mechanistic fragmentation of macroscopic particles that remain undetected because of their very small size (<2.7 nm, diameter). The current state-of-the-art particle measuring system can only measure particles in the 3 nm diameter range using an Ultrafine Condensation Particle Counter (TSI Inc., St. Paul, MN). The $-(\text{H}_2\text{SO}_4)_2 \cdot 2\text{H}_2\text{O}-$ chain would simply grow on the various exposed sites of these ultrafine particles.

5. Conclusion

The structures, energetics, spectra, dipoles and rotational constants of $(\text{H}_2\text{SO}_4)_2 \cdot n\text{H}_2\text{O}$ ($n = 0-6$) have been reported. The structures of $(\text{H}_2\text{SO}_4)_2 \cdot n\text{H}_2\text{O}$ ($n = 0-6$) are primarily held together by hydrogen bonds. Although the initial formation of $(\text{H}_2\text{SO}_4)_2 \cdot n\text{H}_2\text{O}$ ($n = 0-6$) from $\text{H}_2\text{SO}_4 \cdot n\text{H}_2\text{O}$ and H_2SO_4 is spontaneous, it has been kinetically and thermodynamically shown that it is generally not possible due to the high dehydration rate. Reasons have been given to allow various reactions that can overcome the initial reaction steps, but further study of these reasons is still needed to give a more appropriate explanation. A chemical mechanism is given to explain the

numerous measurements of stratospheric aerosols that are composed of 75% H₂SO₄ and 25% H₂O. The chemical mechanism explains the experimental measurements by a chain growth mechanism of H₂SO₄ and H₂O.

Acknowledgements

Support from the Biological/Chemical Oceanography Program, Ocean, Atmosphere and Space Department of the Office of Naval Research (award #N00014-92-J-1281).

References

- [1] A.W. Castleman Jr, R.G. Keesee, *Ann. Rev. Earth Planet Sci.* 9 (1981) 227.
- [2] A.W. Castleman Jr, *Space Sci. Rev.* 15 (1974) 547.
- [3] P. Mirabel, J.L. Katz, *J. Chem. Phys.* 60 (1974) 1138.
- [4] A.D. Clarke, *J. Geophys. Res.* 98 (1993) 20.
- [5] K.S. Carslaw, T. Peter, S.L. Clegg, *Rev. Geophys.* 35 (1997) 125.
- [6] W.J. Shugard, R.H. Heist, H. Reiss, *J. Chem. Phys.* 61 (1974) 5298.
- [7] K.D. Perry, P.V. Hobbs, *J. Geophys. Res.—Atmos.* 99 (1994) 22 803.
- [8] D.A. Hegg, *Geophys. Res. Lett.* 17 (1990) 2165.
- [9] P. Hamill, C.S. Kiang, R.D. Cadle, *J. Atmos. Sci.* 34 (1976) 150.
- [10] P. Hamill, O.B. Toon, R.P. Turco, *J. Geophys. Res.* (1990) 417.
- [11] P.H. McMurry, S.K. Friedlander, *Atmos. Environ.* 13 (1979) 1635.
- [12] W.A. Hoppel, *Atmos. Environ.* 21 (1987) 1.
- [13] L.M. Russell, S.N. Pandis, J.H. Seinfeld, *J. Geophys. Res.—Atmos.* 99 (1994) 20 989.
- [14] S.M. Kreidenweis, J.E. Penner, F. Yin, J.H. Seinfeld, *Atmos. Environ.* 25A (1991) 2501.
- [15] D.A. Hegg, L.F. Radke, P.V. Hobbs, *J. Geophys. Res.* 95 (1990) 13 917.
- [16] S.M. Kreidenweis, J.H. Seinfeld, *Atmos. Environ.* 22 (1988) 283.
- [17] P.H. McMurry, *J. Colloid Interface Sci.* 78 (1980) 513.
- [18] G.E. Shaw, *Atmos. Environ.* 23 (1989) 2841.
- [19] R.C. Easter, L.K. Peters, *J. Appl. Meteorol.* 33 (1994) 775.
- [20] M.J. Molina, R. Zhang, P.J. Wooldridge, J.R. McMahon, J.E. Kim, H.Y. Chang, K.D. Beyer, *Science* 261 (1993) 1418.
- [21] T. Koop, K.S. Carslaw, *Science* 272 (1996) 1638.
- [22] R.Y. Zhang, M.T. Leu, L.F. Keyser, *J. Phys. Chem.* 98 (1994) 13 563.
- [23] R. Zhang, J.T. Jayne, M.J. Molina, *J. Phys. Chem.* 98 (1994) 867.
- [24] A.R. Bandy, J.C. Ianni, *J. Phys. Chem. A* 102 (1998) 6533.
- [25] J.M. Rosen, *J. Appl. Meteorol.* 10 (1971) 1044.
- [26] O.B. Toon, J.B. Pollack, *J. Geo. Res.* 78 (1973) 7051.
- [27] A.D. Becke, *J. Chem. Phys.* 98 (1993) 5648.
- [28] M.J. Frisch, G.W. Trucks, H.B. Schlegel, P.M.W. Gill, B.G. Johnson, M.A. Robb, J.R. Cheeseman, T. Keith, G.A. Petersson, J.A. Montgomery, K. Raghavachari, M.A. Al-Laham, V.G. Zakrzewsk, J.V. Ortiz, J.B. Foresman, J. Cioslowski, B.B. Stefanov, A. Nanayakkara, M. Challacombe, C.Y. Peng, P.Y. Ayala, W. Chen, M.W. Wong, J.L. Andres, E.S. Replogle, R. Gomperts, R.L. Martin, D.J. Fox, J.S. Binkley, D.J. Defrees, J. Baker, J.P. Stewart, M. Head-Gordon, C. Gonzalez, J.A. Pople, Gaussian, Inc., Pittsburgh, PA, 1995.
- [29] M. Sodupe, A. Oliva, J. Bertran, *J. Phys. Chem.* 101 (1997) 9142.
- [30] J. Lundell, Z. Latajka, *J. Phys. Chem.* 101 (1997) 5004.
- [31] L. Gonzalez, O. Mo, M. Yanez, *J. Comp. Chem.* 18 (1997) 1124.
- [32] R. Soliva, M. Orozco, F.J. Luque, *J. Comp. Chem.* 18 (1997) 980.
- [33] J.J. Novoa, C. Sosa, *J. Phys. Chem.* 99 (1995) 15 837.
- [34] C.W. Bauschlicher Jr, *Chem. Phys. Lett.* 246 (1995) 40.
- [35] R.M. Minyaev, A.G. Starikov, *Zh. Neorg. Khim.* 42 (1997) 2078.
- [36] R.C. Weast, *Handbook of Chemistry and Physics*, CRC Press, Cleveland, OH, 1973.
- [37] R.J. Weber, P.H. McMurry, L. Mauldin, D.J. Tanner, F.L. Eisele, F.J. Brechtel, S.M. Kreidenweis, G.L. Kok, R.D. Schillawski, D. Baumgardner, *J. Geo. Res.* 103 (1998) 16 385.
- [38] R.J. Weber, J.J. Marti, P.H. McMurry, F.L. Eisele, D.J. Tanner, A. Jefferson, *J. Geophys. Res.—Atmos.* 102 (1997) 4375.
- [39] R.J. Weber, P.H. McMurry, *J. Geophys. Res.—Atmos.* 101 (1996) 14 767.
- [40] R.J. Weber, P.H. McMurry, F.L. Eisele, D.J. Tanner, *J. Atmos. Sci.* 52 (1995) 2242.
- [41] F.L. Eisele, D.J. Tanner, *J. Geophys. Res.—Atmos.* 98 (1993) 9001.
- [42] J.A. Dean, *Lange's Handbook of Chemistry*, McGraw-Hill, New York, 1985.
- [43] J.C. Ianni, Kintecus, <ftp://ccl.osc.edu/pub/chemistry/software/MS-DOS/kintecus/1996>.
- [44] M.C. Rovira, J.J. Novoa, M.H. Whangbo, J.M. Williams, *Chem. Phys.* 200 (1995) 319.
- [45] A.P. Scott, L. Radom, *J. Phys. Chem.* 100 (1996) 16 502.
- [46] R.G. Gilbert, S.C. Smith, *Theory of Unimolecular and Recombination Reactions*, Blackwell Scientific Publications, Oxford, 1990.
- [47] J.T. Jayne, U. Poschl, Y-m. Chen, D. David, L.T. Molina, D.R. Worsnop, C.E. Kolb, M.J. Molina, *J. Phys. Chem. A* 101 (1997) 10 000.